

Numerical modelling of an oil spill in the northern Adriatic

doi:10.5697/oc.54-2.143
OCEANOLOGIA, 54 (2), 2012.
pp. 143–173.

© *Copyright by*
Polish Academy of Sciences,
Institute of Oceanology,
2012.

KEYWORDS

Oil spill
Numerical model
Northern Adriatic

GORAN LONČAR¹
NENAD LEDER²
MARIN PALADIN¹

¹ Water Research Department,
University of Zagreb,
Kačićeva 26, Zagreb 10000, Croatia;

e-mail: goran.loncar@grad.hr, marin.paladin@grad.hr

² Hydrographic Institute of the Republic of Croatia,
Zrinsko-Frankopanska 161, Split 21000, Croatia;

e-mail: nenad.leder@hhi.hr

Received 21 December 2011, revised 15 March 2012, accepted 5 April 2012.

Abstract

Hypothetical cases of oil spills, caused by ship failure in the northern Adriatic, are analysed with the aim of producing three-dimensional models of sea circulation and oil contaminant transport. Sea surface elevations, sea temperature and salinity fields are applied as a forcing argument on the model's open boundaries. The Aladin-HR model with a spatial resolution of 8 km and a time interval of 3 hours is used for atmospheric forcing. River discharges along the coastline in question are introduced as point source terms and are assumed to have zero salinity at their respective locations. The results of the numerical modelling of physical oceanography parameters are validated by measurements carried out in the 'Adriatic Sea monitoring programme' in a series of current meter and CTD stations in the period from 1 January 2008 to 15 November 2008.

The oil spill model uses the current field obtained from a circulation model. Besides the convective dispersive transport of oil pollution (Lagrangian model of discrete particles), the model takes into account a number of reactive processes

The complete text of the paper is available at <http://www.iopan.gda.pl/oceanologia/>

such as emulsification, dissolution, evaporation and heat balance between the oil, sea and atmosphere. An actual event took place on 6 February 2008, when the ship 'Und Adriyatik' caught fire in the vicinity of the town of Rovinj (Croatia) en route from Istanbul (Turkey) to Trieste (Italy). At the time the fire broke out, the ship was carrying around 800 tons of oil. Thanks to the rapid intervention of the fire department, the fire was extinguished during the following 12 hours, preventing possible catastrophic environmental consequences. Based on this occurrence, five hypothetical scenarios of ship failure with a consequent spill of 800 tons of oil over 12 hours were analysed. The main distinction between the simulated scenarios is the time of the start of the oil spill, corresponding to the times when stronger winds were blowing ($> 7 \text{ m s}^{-1}$) with a minimum duration of 24 h within the timeframe. Each scenario includes a simulation of oil transport for a period of two months after the beginning of the oil spill.

The results show that the coastal belt between the towns of Poreč and Rovinj is seriously exposed to an oil pollution load, especially a few days after a strong and persistent bora (NE wind).

1. Introduction

The Adriatic Sea is a deeply indented gulf of the Mediterranean (ca 800 km long and 200 km wide); it is classified as a semi-enclosed sea. It is situated between the Apennine and Balkan peninsulas, at longitudes between $12^{\circ}15'E$ and $19^{\circ}45'E$, and latitudes between $39^{\circ}45'N$ and $45^{\circ}45'N$ (Figure 1). The southern border of the Adriatic Sea crosses the Strait of Otranto in a line running from the mouth of the River Buttrinto ($39^{\circ}44'$) in Albania to Cape Karagol in Corfu, across this island to Cape Kephali (these two capes are at latitude $39^{\circ}45'N$) and on to Cape Santa Maria di Leuca in Italy (IHO – International Hydrographic Organization 1953). The shallowest part of the Adriatic Sea is the northern Adriatic, a closed basin where, to the north of a line joining Pula and Ancona, depths do not exceed 50 m.

The surface circulation of the Adriatic Sea is regarded as a cyclonic meander comprising a northerly flow along the eastern coast and a southerly outgoing flow along the western coast (Orlić et al. 1992). A review of the Adriatic Sea circulation can be found in e.g. Orlić et al. (1992) and Cushman-Roisin et al. (2001). The Adriatic circulation depends strongly on the characteristics of air-sea fluxes of momentum, heat and water at the air-sea interface (Cushman-Roisin et al. 2001). In general, the resultant surface circulation in the Adriatic can be explained as a modification of gradient currents under the influence of tides and blowing winds.

For the purposes of this paper special attention will be given to the surface circulation of the northern Adriatic, especially to departures from its general circulation pattern. The double-gyre response of the northern

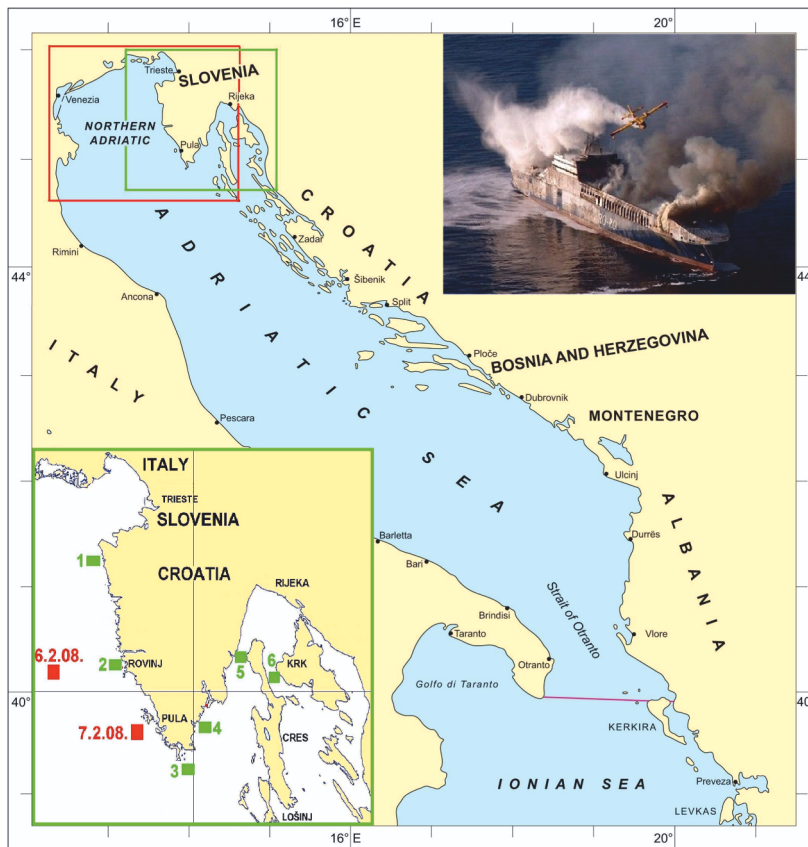


Figure 1. Map of the Adriatic Sea, positions of the ADCP/CTD stations (green rectangles numbered from 1 to 6), positions of ‘Und Adriyatik’ on 6 and 7 February (red rectangles) and the area covered with a numerical model spatial domain (indicated with red borderlines)

Adriatic to intense bora winds (a cyclonic gyre north of the Po Delta – Rovinj line and an anticyclonic gyre to the south; Figure 2) has been described by a number of authors, e.g. Zore-Armanda & Gačić (1987), who analysed current meter data, and Orlić et al. (1994), who applied a numerical model.

The Istrian Coastal Countercurrent (ICCC) and its year-on-year variability is another interesting phenomenon in the northern Adriatic, observed (e.g. Supić et al. 2000) and reproduced by numerical models (e.g. Cushman-Roisin & Korotenko 2007). A southerly current along the Istrian coast, the ICCC usually appears in the summer season; this is a current reversal in comparison with the general circulation. While Supić et al. (2000) correlated the ICCC with air-sea fluxes and the River Po’s discharge over

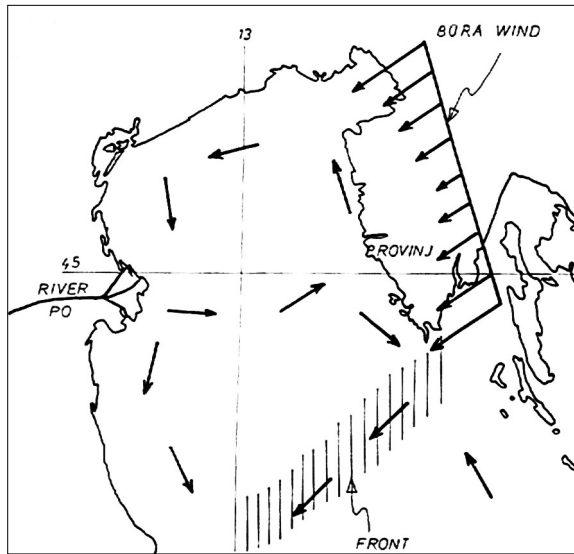


Figure 2. Schematic representation of the bora wind field and the water circulation in the northern Adriatic, with the position of the frontal zone indicated by hatching (after Zore-Armanda & Gačić 1987)

a period of one month or longer prior to the current reversal, Cushman-Roisin & Korotenko (2007) suggested that two ingredients were necessary for the establishment of the ICC: first, a preconditioning phase ending with different water characteristics on the eastern and western shores of Istria, and, second, a bora event bringing the latter water into contact with the former.

It should be noted that a permanent operational oceanographic system with both monitoring components (observation/modelling) in place has not yet been established in Croatia. In the last decade there have been some periodic and intensive monitoring programmes with the participation of Croatian institutions, covering the entire area of the Adriatic (ADRICOSM Project (Acta Adriatica 2006); Adriatic Sea Monitoring Programme (Androćec et al. 2009)), or only parts of the Adriatic basin (MAT Project (Science of the Total Environment 2005); the Croatian National Monitoring Programme (www.cim.irb.hr/projekti/projekt-jadran/)). For the purpose of detecting the spread of oil spills within the Adriatic area, the SAR/GIS monitoring system (Morović & Ivanov 2011) is already in place but has not been followed up with numerical model implementation at operational level for forecasting and strategic decision-making.

In the early morning hours of 6 February 2008, a Turkish freighter caught fire in the Adriatic Sea 13 nautical miles west of the town of Rovinj

(Figure 1). An SOS was sent at 04:04 hrs local time. The 193 m long ship was sailing from Istanbul in Turkey to Trieste in Italy and was carrying 200 trucks and nine tons of hazardous material, in addition to a few hundred tons of ship fuel, causing fears of environmental damage. As the fire had started inside the ship (Figure 1), there was no way of extinguishing it from the outside.

Motivated by this incident, we conducted a numerical analysis with hypothetical scenarios of oil spreading resulting from a 12-hour continuous crude oil spill from a stationary ship at 18.5 kg s^{-1} , reaching a total amount of 800 tons. Therefore, the present study includes several steps: a) running a numerical model that defines a three-dimensional unsteady and non-uniform sea current, temperature and salinity fields for the continuous period 1 January–15 November 2008; b) running an oil pollution transport model based on reactive and dispersive processes, also accounting for the intense surface horizontal spreading in the first stage after the oil spill.

Analysis of wind data for the position of the ‘Und Adriyatik’ when it failed (Figure 1) during the sea circulation simulation period (1 January–15 November 2008) shows seven situations in which the wind, regardless of its direction, had a speed higher than 7 m s^{-1} continuously for 24 hours. The onset of wind conditions satisfying the aforementioned criteria were at the following times and dates: 18:00 hrs, 11 January 2008; 15:00 hrs, 7 February 2008; 15:00 hrs, 4 March 2008; 06:00 hrs, 13 July 2008; 18:00 hrs, 13 September 2008; 21:00 hrs, 25 September 2008; 18:00 hrs, 28 October 2008; as such they could be adopted as the hypothetical times when the oil spill occurred. The analysis of the spreading oil in each hypothetical scenario extends for two months after the start of the spill. Because of the lack of data on wind situations after 15 November 2008, the last two scenarios starting on 25 September 2008 and 28 October 2008 are not covered by numerical simulations.

Explanations regarding the modelling approach are given in part 2. Validation of the numerical model results through comparisons with the measurements and results of the oil spreading modelling is given in part 3. The conclusions of the study are listed in part 4.

2. Material and methods

A sea circulation model was initially used for the purpose of the following oil transport simulations. In the analysis of sea circulation, the three-dimensional Mike 3 numerical model (DHI 2005) was used. The mathematical foundation of Mike 3 is the mass conservation equation, the Reynolds-averaged Navier-Stokes equations, including the effect of

turbulence and variable density, together with the conservation equations for salinity and temperature. The hydrodynamic module of Mike 3 makes use of the so-called Alternating Direction Implicit (ADI) technique to integrate equations for mass and momentum conservation in the space-time domain. The equation matrices were resolved by a Double Sweep (DS) algorithm, discretized on an Arakawa C-grid with second-order accuracy. The 3D Quickest-Sharp scheme was used for the analysis of the transported scalar fields.

The model spatial domain (Figures 1 and 3) was discretized using a finite difference mesh with equidistant spatial increments $\Delta x = \Delta y = 500$ m in the horizontal and $\Delta z = 2$ m in the vertical direction. The calculation time step used in the numerical integration was set to $\Delta t = 60$ s. The simulation period covered the time span from 1 January 2008 to 15 November 2008. The model output data sets included sea currents (u , v components), sea temperature (T) and salinity (S).

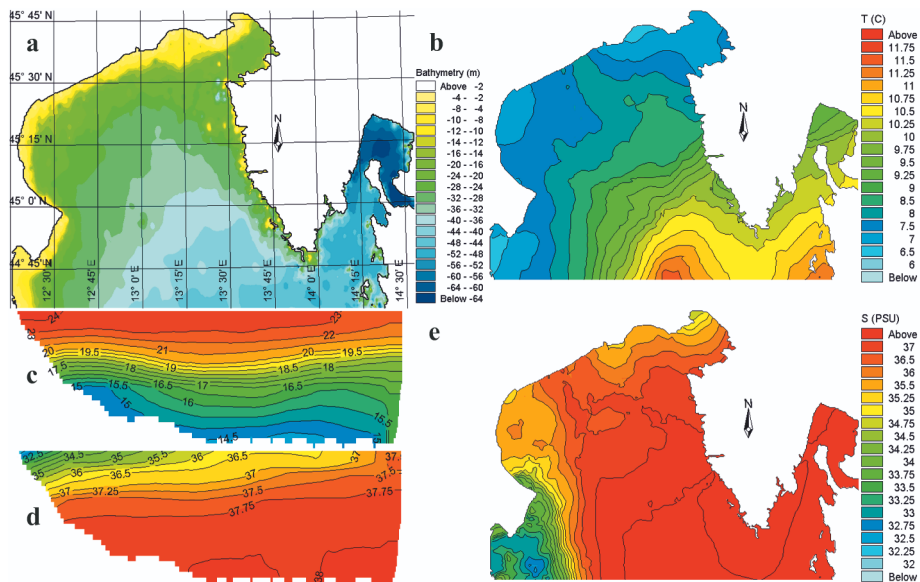


Figure 3. Area covered by the numerical model spatial domain with bathymetry (a), sea temperature (c) and salinity (d) distribution in the transect of the model's open boundary for the beginning of July (according to Galos 2000), and surface fields for sea temperature (b) and salinity (e) for the beginning of January (according to Galos 2000)

The sea level dynamics on the model open boundaries were synthesized using seven major tidal constituents: M2, S2, K2, N2, K1, O1 and P1 (Janeković et al. 2003, Janeković & Kuzmić 2005, Janeković & Sikirić-

Dutour 2007). The influences of river inflows along the shoreline under scrutiny were introduced with daily average discharges according to Raicich (1996). Salinity at the positions of the river mouths was parameterized with a value of 0 PSU. Bottom freshwater springs were also taken into account with positions and intensity defined within the scope of the ‘Adriatic Sea monitoring programme’ (Andročec et al. 2009).

For atmospheric forcing, Mike 3 utilizes the output data from the Aladin-HR prognostic atmospheric model (Members of the Aladin International Team 1997, Courtier et al. 1991, Cordoneanu & Geleyn 1998, Brzović 1999, Brzović & Strelec-Mahović 1999, Ivatek-Šahdan & Tudor 2004) with a spatial resolution of 8 km and a temporal resolution of 3 hours. The bulk relation used includes wind speed and direction, air pressure, air temperature, relative humidity, cloudiness and short-wave radiation.

Numerical integrations with the Mike 3 model started on 1 January 2008 and were initialized with mean winter seasonal fields of temperature and salinity at standard oceanographic levels from the Dartmouth Adriatic Data Base (DADB). The DADB data base is constructed from two existing data sets (Galos 2000): the Mediterranean Oceanographic Data Base and the Adriatic Sea Temperature, Oxygen and Salinity Data Set (Cushman-Roisin et al. 2007). Interpolation and extrapolation of T and S values from the data sets on the numerical nodes of the Mike 3 model (Figure 3) were performed with the use of objective analysis (Bretherton & Fauday 1976).

The turbulent closure model used within Mike 3 relies on a k - ε formulation in the vertical direction (Rodi 1987) and in the horizontal direction (Smagorinsky 1993). In the model parameterization we used the very same values as in the previously completed study (Andročec et al. 2009), with regard to the sea circulation, where the same Mike 3 numerical model system was applied to the same spatial domain. Sensitivity analysis and more detailed validation of the numerical model results were also included in the work by Andročec et al. (2009). In addition to the values adopted from previous studies (dispersion coefficients for T , S , k and ε), the model’s parameterization relies on literature-referenced values without their overall influence on the numerical model results being examined: 0.00123 for the wind friction coefficient (Wu 1994), $a = 0.25$ and $b = 0.52$ for the correlative coefficients in Angstrom’s law (Zaninović et al. 2008), 0.5 and 0.9 for the wind constant and the evaporation coefficient in Dalton’s law respectively. The heat flux absorption profile in the short-wave radiation is described by a modified version of Beer’s law. The values adopted were 0.2 for the energy absorption coefficient in the surface layer and 0.1 for the light decay coefficient in the vertical direction.

The convective-dispersive component of the oil transport module was established by means of the Lagrangian discrete particles approach. The displacement of each Lagrangian particle is given by the sum of an advective deterministic and a stochastic component, the latter representing the chaotic nature of the flow field, the sub-grid turbulent dispersion. The movement of Lagrangian particles due to advection in a three-dimensional current field is described by the following ordinary differential equation:

$$\frac{d\vec{x}_p}{dt} = \vec{v}(\vec{x}_p, t), \quad (1)$$

where \vec{v} is the vector velocity with components (u, v, w) in the x, y and z directions, and \vec{x}_p is the coordinate of the particle in the three directions. The velocity field relies on the results of the current field, obtained by simulation with the Mike 3 sea circulation model. Turbulent dispersion can be defined as a random and independent Markov process (Gardiner 1985), where the influence of turbulence on particle movement is modelled with a random walk methodology. The Langevin non-linear equation is used for describing the tracer position (Gardiner 1985, Kloeden & Platen 1999):

$$\frac{d\vec{x}(t)}{dt} = \vec{A}(\vec{x}, t) + \mathbf{B}(\vec{x}, t)\vec{\xi}(t), \quad (2)$$

where $\vec{A}(\vec{x}, t)$ represents the vector of the deterministic part of the flow field (transport by the Mike 3 current field). The second term is a stochastic or diffusion term consisting of the tensor $\mathbf{B}(\vec{x}, t)$, characterizing random motion, and the random number vector $\vec{\xi}(t)$ with values between 0 and 1. Equation (1) is equivalent to the stochastic differential equation:

$$d\vec{x}(t) = \vec{A}(\vec{x}, t)dt + \mathbf{B}(\vec{x}, t)d\vec{W}(t), \quad (3)$$

where $d\vec{W}$ is the random Wiener process with the properties of the zero mean and mean square value proportional to dt . The unknown parameters \vec{A} and \mathbf{B} are determined by the Fokker-Planck equation associated with equation (3), which in the three-dimensional version reads:

$$d\vec{x}(t) = \begin{pmatrix} u(\vec{x}, t) \\ v(\vec{x}, t) \\ w(\vec{x}, t) \end{pmatrix} dt + \begin{bmatrix} \sqrt{2D_X} & 0 & 0 \\ 0 & \sqrt{2D_Y} & 0 \\ 0 & 0 & \sqrt{2D_Z} \end{bmatrix} \begin{pmatrix} Z_1 \\ Z_2 \\ Z_3 \end{pmatrix} \sqrt{dt}, \quad (4)$$

where Z_1, Z_2, Z_3 are the independent random numbers normally distributed around a zero mean value and unit variance, and D_1, D_2 and D_3 are the diffusive coefficients. Particles in a Lagrangian discrete parcels model are most of the time situated at off-grid points. The bilinear interpolation is used to interpolate the velocities in space.

Processes that alter the oil's characteristics begin immediately after an oil spill on the sea surface. Some of these processes, such as evaporation, emulsification, dissolution, photo-oxidation and biodegradation, are primarily controlled by the characteristics of the oil itself (Korotenko et al. 2001, 2004, 2010). Different processes dominate during the time elapsing from the beginning of the spill. Evaporation is the most intense immediately after the spill, subsiding gradually over a period of 1 000 hours (Wheeler 1978). Emulsification continuously increases its effect in the first 100 hours after the spill and then weakens in the subsequent period up to 1 000 hours (Wheeler 1978). Dissolution also takes place soon after the spill (1 hour), gradually increasing over a period of 50 hours, and weakening in the next 1 000 hours (Wheeler 1978). Photo-oxidation is activated shortly after the spill, and makes a contribution over an extended period of 10 000 hours but with a generally less pronounced impact than the previously mentioned factors (Wheeler 1978). Biodegradation and sinking come into play only at a later stage, 600 hours after the occurrence of the oil spill (Wheeler 1978). In addition to these processes, a very important parameter in the overall mechanism of oil pollution transport is the three-dimensional flow field with a corresponding dispersive mechanism that is continually present. In this study, the main focus is on the dominant processes that cause significant short-term changes in oil characteristics over time: spreading, evaporation, dispersion and emulsification.

The initial horizontal expansion (spreading) of an oil slick due to mechanical forces such as gravity, inertia, viscous and interfacial tension is dealt with according to the methodology shown in Fay (1969) and the modification proposed by Mackay et al. (1980). The rate of spreading is given as (Mackay et al. 1980):

$$\frac{dA}{dt} = K_S A^{1/3} \left(\frac{V}{A} \right)^{4/3}, \quad (5)$$

where K_S is a parameter of value 150 s^{-1} , A is the oil slick area [m^2] and V is the volume of the oil slick [m^3]. This formula is based on the following assumptions: oil is regarded as a homogeneous mass, the slick spreads out as a thin, continuous layer in a circular pattern and there is no loss of mass from the slick. The initial area of the spilled oil A_0 is determined according to Fay (1969):

$$A_0 = \pi \frac{k_2^4}{k_1^2} \left(\frac{\Delta g V_0^5}{v_w} \right)^{1/6}, \quad (6)$$

where g is the acceleration due to gravity [m s^{-2}], $\Delta = (\rho_w - \rho_0)/\rho_w$ with ρ_w being the seawater density [kg m^{-3}], ρ_0 is the density of fresh oil [kg m^{-3}],

V_0 is the initial volume of the slick, ν_w is the kinematic viscosity of water [$\text{m}^2 \text{s}^{-1}$] and k_1 , k_2 are constants with respective values of 0.57 and 0.725 (Flores et al. 1998).

Evaporation processes are modelled according to the methodology proposed by Mackay et al. (1980), taking into account the influence of oil composition, air and sea temperatures, spill area, wind speed, solar radiation and slick thickness. In addition, the following assumptions are made: no diffusion limitation exists within the oil film; oil forms an ideal mixture; the partial pressures of the components in the air, compared to the vapour pressure, are negligible. The rate of evaporation is then calculated using the following equation:

$$E_i = \frac{K_{ei} P_i^{SAT}}{RT} \frac{M_i}{\rho_i} X_i, \quad (7)$$

where E_i is the rate of evaporation of the oil fraction i , K_{ei} is the mass-transfer coefficient of the oil fraction i [m s^{-1}], P_i^{SAT} is the vapour pressure of the oil fraction i , R is the gas constant [$8.314 \text{ J K}^{-1} \text{ mol}^{-1}$], T is temperature [K], M_i is the molecular weight of the oil fraction i [kg mol^{-1}], ρ_i is the density of the oil fraction i [kg m^{-3}], X_i is the mole ratio of fraction i to the oil mixture [1], i is the subscript referring to the properties of component i . The estimate of K_{ei} is also based on Mackay et al. (1980):

$$K_{ei} = 0.0292 A^{0.045} S_{ci}^{-2/3} U_w^{0.78}, \quad (8)$$

where S_{ci} is the Schmidt number for fraction i [1], and U_w is the wind speed 10 m above the surface [m s^{-1}].

The process of emulsification is treated according to the empirical expressions defined in IKU (1984). The change in water content Y_W with time is expressed by:

$$\frac{dY_W}{dt} = F_1 \frac{(1 + U_w)^2}{\mu} (Y_{W_{\max}} - Y_W) - F_2 \frac{1}{C_A C_W \mu} Y_W, \quad (9)$$

where $Y_{W_{\max}}$ is the maximum water content in the emulsion [-], Y_W is the actual water content, μ is the oil viscosity [Pas], C_W is the content of wax in the oil [wt%], C_A is the content of asphaltenes in the oil [wt%], F_1 [kg m^{-3}] and F_2 [kg(wt\%) s^{-1}] are emulsification constants. In model simulations the values of 0.85, 5.7, 0.05, 5E-7 and 1.2E-5 are adopted for $Y_{W_{\max}}$, C_W , C_A , F_1 and F_2 respectively. The first term on the right-hand side of equation 9 defines the rate of water uptake, indicating an increase with increasing temperature and wind speed. The second term defines the rate of water release and decreases with increasing content of asphaltenes, wax and surfactants in the oil and with increasing oil viscosity.

Vertical transport of oil into the water column can be accomplished by a number of mechanisms, such as dissolution, dispersion, accommodation and sedimentation. The model accounts only for natural dispersion and treats it as an entrainment process, whereby the formation of an oil-in-water emulsion is a consequence of increased turbulence in the surface layer.

According to Mackay et al. (1980), vertical dispersion can be estimated as the fraction of the sea surface that is dispersed in the water column per unit time, using the following equation:

$$D_0 = D_D D_{EN}; \quad D_D = \frac{0.11(1 + U_w)^2}{3600}; \quad D_{EN} = \frac{1}{1 + 0.5\mu h\gamma_{EN}}, \quad (10a, b, c)$$

where D_D accounts for the dispersed fraction of the sea surface into the water column per second, and D_{EN} accounts for the fraction of the dispersed oil not returning to the surface oil slick. The symbol h stands for the oil slick thickness [m], and γ_{EN} is the oil-water interfacial tension [N m^{-1}] for the entrainment parameterization. The rate of upwelling of dispersed oil droplets is calculated from

$$\frac{dV}{dt} = \frac{0.11(1 + U_{w-AV})^2}{3600} \left(1 - \frac{1}{1 + 0.5\mu h\gamma_{EN}} \right). \quad (11)$$

The term U_{w-AV} in equations 10 and 11 represents the spatially averaged wind speed from a 2D wind field that is also used in the sea circulation model. However, such a simplification neglects inhomogeneous surface wave breaking, and consequently, induced inhomogeneous turbulence in the sea surface layer (inhomogeneous intensity of natural dispersion).

The rate of oil entrainment from the slick to the water column can be scaled as (Tkalich & Chan 2002):

$$\lambda_{OW} = \frac{k_b \omega \gamma H_S}{16\alpha L_{OW}}, \quad (12)$$

where λ_{OW} is the entrainment rate [s^{-1}], k_b is the coefficient calculated from experiments [-], ω is the wave frequency [1 s^{-1}], γ is the white-capping dimensionless damping coefficient $\gamma = 1E - 5\omega(\rho g H_S/16)^{0.25}$ according to Hasselmann (1974) [-], H_S is the significant wave height [m], α is the dimensionless scaling factor [-] and L_{OW} is the vertical length-scale parameter [m].

Adopting the values of 0.4 for k_b (Lamarre & Melville 1991) and 1.5 for α (Delvigne & Sweeney 1988), and knowing the spatial averages of significant wave heights H_S and wave spectra peak periods T_P in the model domain, one can calculate and compare the time series of λ_{OW} and D_D .

Numerical modelling of wind wave generation in the entire Adriatic area for the period 1 January–15 November 2008 was carried out on the basis

of the same wind field as applied in the model of sea circulation and oil transport (Lončar et al. 2010).

The results were validated by comparison with wave-rider records (Lončar et al. 2010). Model results of the inhomogeneous and non-stationary H_S and T_P fields were transferred to the finite difference grid used in the model of oil transport with the aim of bilinear interpolation. Subsequently, the time series of spatially averaged H_{S-AV} and T_{P-AV} values were calculated along with the corresponding time series for λ_{OW} . The time series for λ_{OW} , obtained using equation 12, and the time series for D_D/ρ_W , obtained using expression 10b, are compared in Figure 4. Using the expression for D_D suggested by Mackay et al. (1980) rather than that of Tkalich & Chan (2002) will result in an average overestimation of the natural dispersion process by 4%.

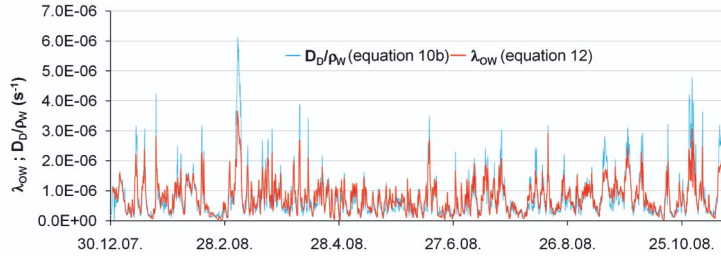


Figure 4. Comparison of time series for λ_{OW} (according to equation (12)) and for D_D/ρ_W (according to equation (10b))

The heat exchange between air and oil, and between oil and sea, is based on the works of Duffie & Beckmann (2006) and Bird et al. (1960). The dependence of viscosity on temperature, aqueous phase participation and evaporation is solved as suggested by CONCAWE (1983) and Hossain & Mackay (1980). The evaporation pressure at an arbitrary temperature was defined according to Yang & Wang (1977) and changes in the fluidization point according to CMFMWOS (1985). The atmospheric and sea properties, relevant to the process of oil transformation, are taken directly from the sea circulation model.

The spilled oil may be deposited along the shoreline and afterwards re-entrained into the water column. Numerical modelling of oil behaviour at the shoreline relies primarily on empirical formulations, because of the very complex processes and interactions involved (Guo & Wang 2009). Incorporating all these factors into the model routine is almost impossible owing to the limited data available (Owens et al. 2008). The oil transport model uses the perfect reflection algorithm in situations where a particle

encounters land, assuming zero kinetic energy loss on impact and equality of the angles of incidence and reflection.

For modelling purposes, the partial constituents of oil are divided into eight fractions; their chemical structure and distillation characteristics are shown in Table 1. The adopted initial temperature of the spilled oil is 25°C in every simulation.

Table 1. The fractions of model heavy crude oil divided by chemical composition, distillation characteristics, densities and percentage participation, used in the numerical simulations (Yang & Wang 1977)

	Fraction	Boiling range T [°C]	Density [kg m ³]	Participation [%]
1	C6–C12 (Paraffin)	69–230	715	6
2	C13–C25 (Paraffin)	230–405	775	30
3	C6–C12 (Cycloparaffin)	70–230	825	15
4	C13–C23 (Cycloparaffin)	230–405	950	5
5	C6–C11 (Aromatic)	80–240	990	4
6	C12–C18 (Aromatic)	240–400	1150	10
7	C9–C25 (Naptheno-aromatic)	180–400	1085	10
8	Residual (incl. heterocycles)	> 400	1050	20

The occurrence of oil pollution due to ship failure is modelled as a continuous and steady input discharge $Q_{\text{spill}} = 18.5 \text{ kg s}^{-1}$ into the model surface layer for a period of 12 hours, resulting in a total amount of 800 tons of spilled oil.

Specifying that 200 Lagrangian particles are released at each time step in the oil transport model $\Delta t = 200 \text{ s}$, and that a constant source flux of 18.5 kg s^{-1} is defined, then each released particle has a mass of 18.5 kg. The thickness of the slick is calculated at the end of a time step Δt by counting the particles in the grid cells and then, for each grid cell, dividing the total volume of the particles present in the cell by the area of the cell.

3. Results and discussion

Calibration of the Mike 3 model is based on the measurement data sets obtained in the ‘Adriatic Sea monitoring programme’, which was conducted in the territorial waters of the Republic of Croatia (Androćec et al. 2009). The Mike 3 results were compared with CTD and ADCP measurements. An overview of the Mike 3 result along with measured temperature and salinity profiles at the corresponding ADCP/CTD station 2 (see Figure 1) is given in Figure 5.

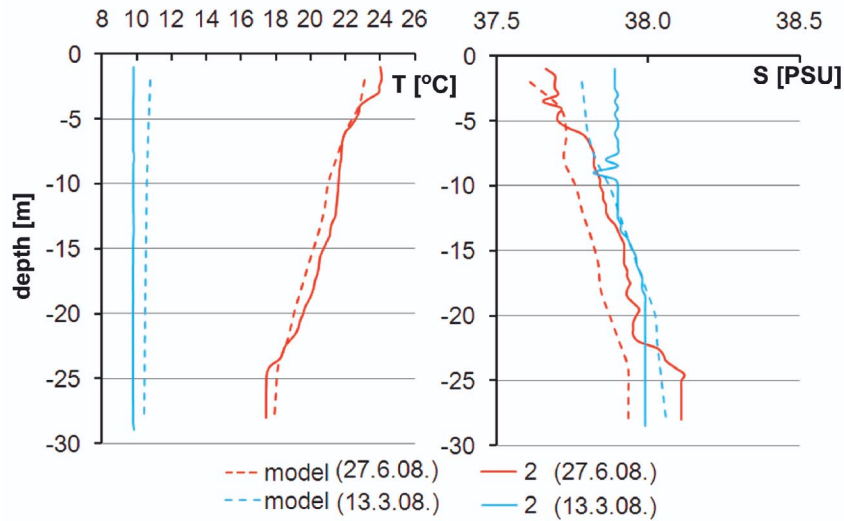


Figure 5. Measured and modelled (Mike 3) sea temperature (left) and salinity (right) along a vertical profile at ADCP/CTD station 2 (see Figure 1) for the spring and summer seasons

The sea temperature obtained with the Mike 3 model is in agreement with the CTD measurements at almost all the monitoring stations. Statistical analysis shows that the RMS error is 0.51°C , the average error (AE) is -0.03°C , while the correlation coefficient is around 0.85 for the 95% confidence interval. In the salinity field, the results are good, the RMS error is 0.43, and the mean error is 0.31 with a correlation coefficient of 0.68. The somewhat lower value of the correlation reflects the poorly known forcing of freshwater in the model (rivers and freshwater bottom springs) through the use of crude climatology values. The most pronounced differences between model and measurement results are seen at stations 5 and 6 (Figure 1), for the previously mentioned reasons. Furthermore, using the referenced values of sea temperature and salinity on the model's open boundary, either via the measurement or the model nesting in the basin-wide Adriatic model, would significantly reduce the differences between the model results and the measurements.

The model results of hourly averaged current velocities in relation to the ADCP measurements at stations 1, 2, 3, 4, 5 and 6 for the time intervals 15 July–15 August 2008 and 1 March–1 April 2008 are given in Figure 6. The average errors (AE) of the calculated values of current velocities using the numerical model in relation to the measured values are shown in Table 2. Figure 7 shows the model current fields for the surface layer, averaged over the months of March, April, July and August 2008.

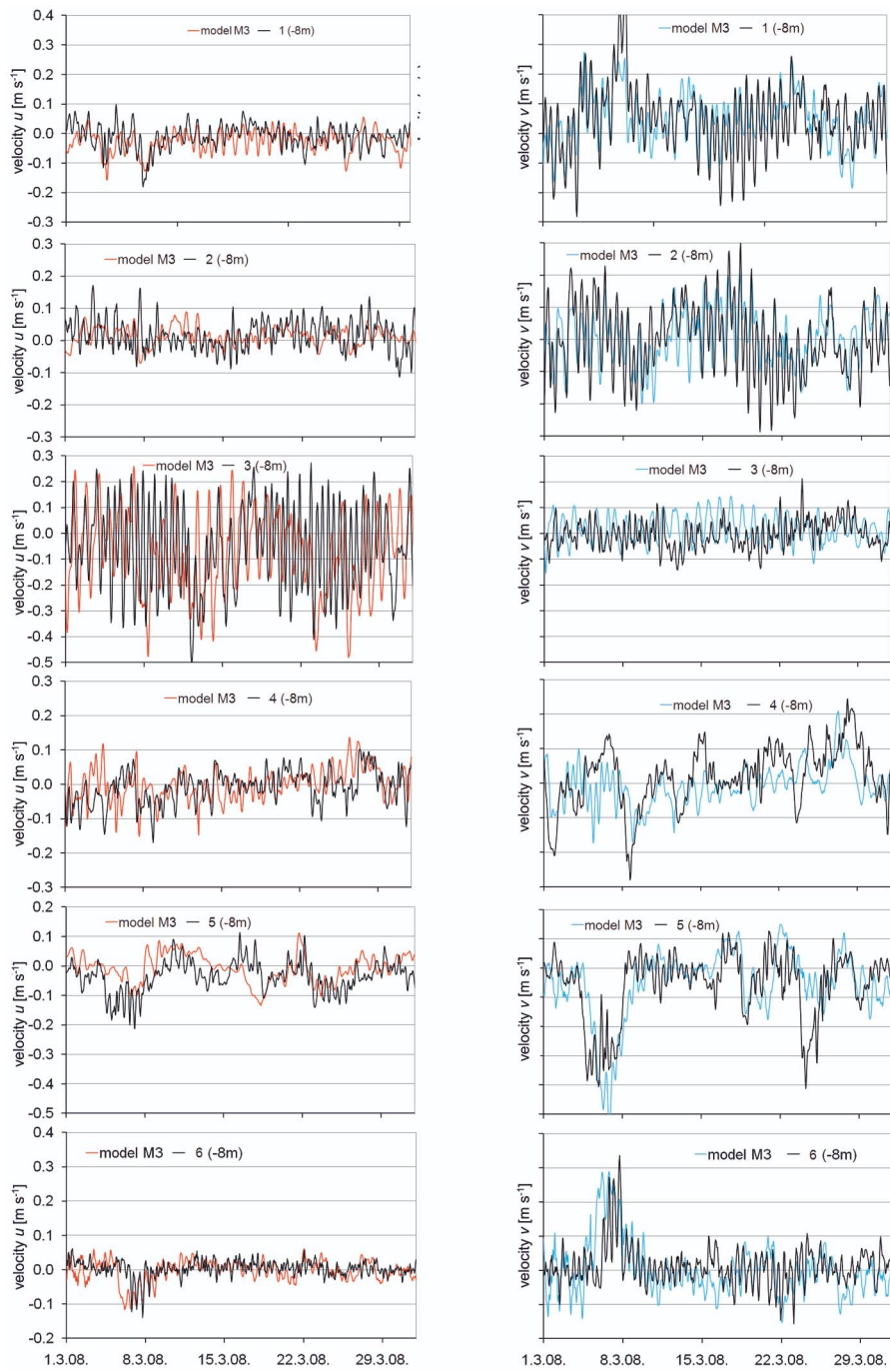


Figure 6. Comparison of measured (current meter stations 1–6) and modelled (Mike 3) hourly averaged current velocities at a depth of 8 m

Table 2. Average errors (AE) for model values of current velocity components (u , v) in relation to the measured values, for ADCP/CTD stations 1 to 6, at a depth of 8 m

ADCP	1	2	3	4	5	6
Depth	8 m	8 m	8 m	8 m	8 m	8 m
AE (u)	-0.018	-0.003	-0.017	0.008	0.025	-0.006
AE (v)	0.002	0.013	0.021	-0.028	-0.005	-0.011

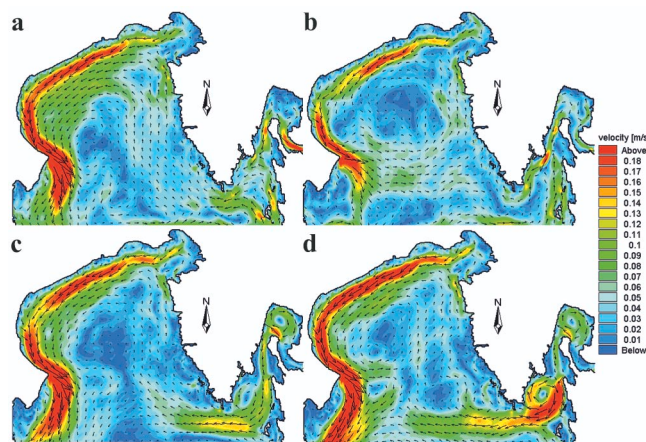


Figure 7. Model current fields for the surface layer (0–2 m depth) averaged over March (a), April (b), July (c) and August (d) 2008

The current velocities obtained with the Mike 3 model are consistent with the measured values for most of the simulation time at all ADCP current meter stations. More reliable model results were obtained for the positions of current meter stations 6, 1, 2 and 5 than for 3 and 4 (Table 2). The better agreement of the model and the measured results at these stations is a consequence of the high energy contained in the tidal signal (see Figure 8), which is also easier to determine and implement on the model boundaries than other forces like gradient currents and weather disturbances. An interesting fact is that the action of the bora wind caused an intensively ‘ascending’ flow towards Rijeka Bay at the position of ADCP monitoring site 4 during the winter period. This transitional phenomenon failed to be registered within the Mike 3 model results. Obviously, the use of a 3 hour and 8 km wind field resolution from the Aladin model introduces some bias directly into the Mike 3 model through erroneous and excessively coarse atmospheric forcing data. Furthermore, the temporal and spatial

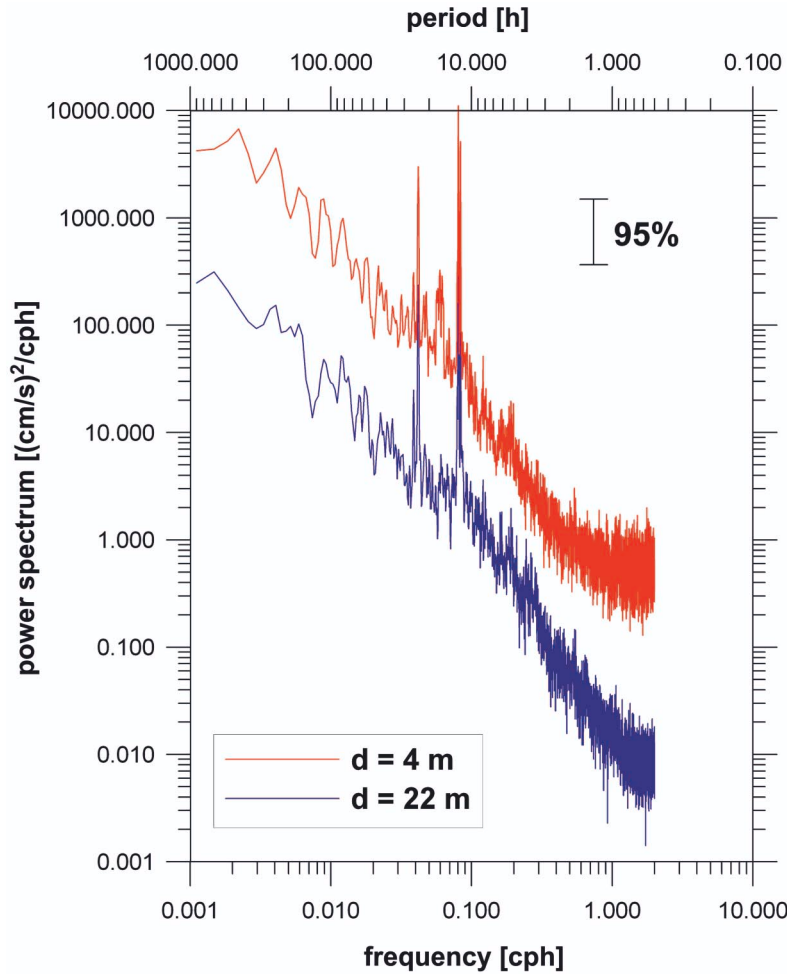


Figure 8. Total current spectrum in subsurface and near-bottom layers at station 1 (from June 2008 to January 2009). Spectral values for the bottom layer (22 m depth, blue) are divided by a factor of 10 to prevent the overlap of spectra. The spectra were determined using the Welch method, with three half-overlapping Hamming windows. The confidence intervals at 95% were calculated from the number of degrees of freedom (21)

dynamics used in the T and S fields at the open boundary transect relies on climatology data sets (Galos 2000), giving information about T and S distribution only on four dates: 1 January 2008, 1 April 2008, 1 July 2008 and 1 October 2008.

Figure 9 shows the time series of wind speed and direction at the position of the ship's failure as well as the symbols for the labelled terms of the hypothetical onset of the oil spill. Figure 10 shows the wind fields for

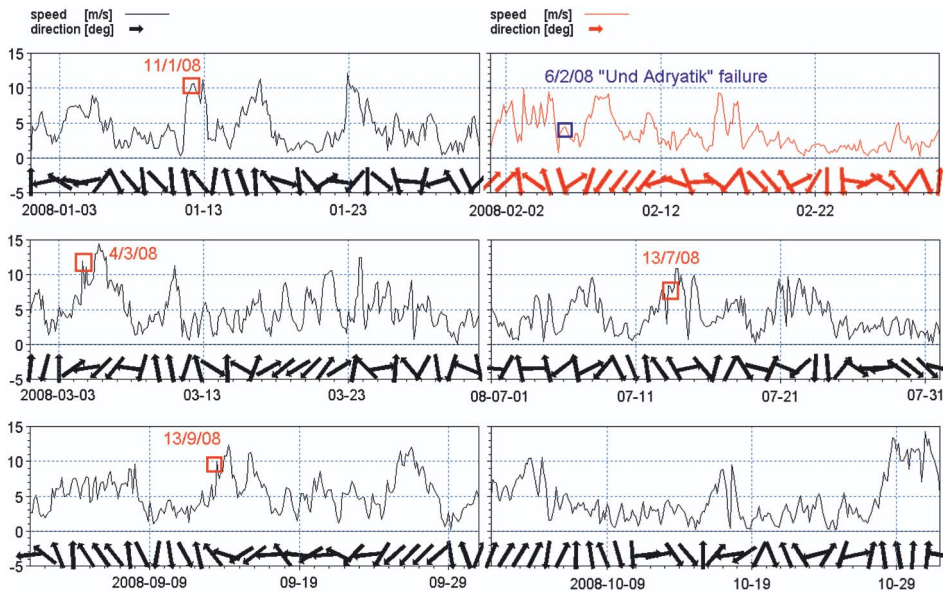


Figure 9. Time series of wind speed and direction at the position of the ship's failure, and labelled times of the onset of the hypothetical oil spills (data on direction and wind speed were obtained from the Aladin-HR numerical atmospheric model)

the model spatial domain during periods shortly after the hypothetical oil spill.

At station 1 ($13^{\circ}29.477\text{E}$, $45^{\circ}24.999\text{N}$) current measurements were performed using an ADCP 600 kHz Workhorse Sentinel unit manufactured by Teledyne RDI, at 9 levels (6 m to 22 m bins) with a vertical spatial resolution of 2 metres, and a sampling interval of 15 minutes. The most significant spectral energies at station 1 (Figure 8) were observed during semidiurnal and diurnal tidal periods, and during long periods (gradient currents and synoptic atmospheric disturbances, periods longer than 40 h). It is interesting that during diurnal tidal periods, the energies of subsurface and near-bottom currents are of the same order of magnitude, while for semidiurnal periods the energy of the subsurface current is an order of magnitude larger. In addition, energy peaks were also detected at 16.8 h, representing the inertial period, and during the period of the fundamental Adriatic seiche (21 h). Subsurface currents (at a depth of 4 m) were somewhat more pronounced than near-bottom currents (22 m depth).

Figures 11 to 15 show the plumes of oil pollution for the 240th and 480th hours after the onset of the spill.

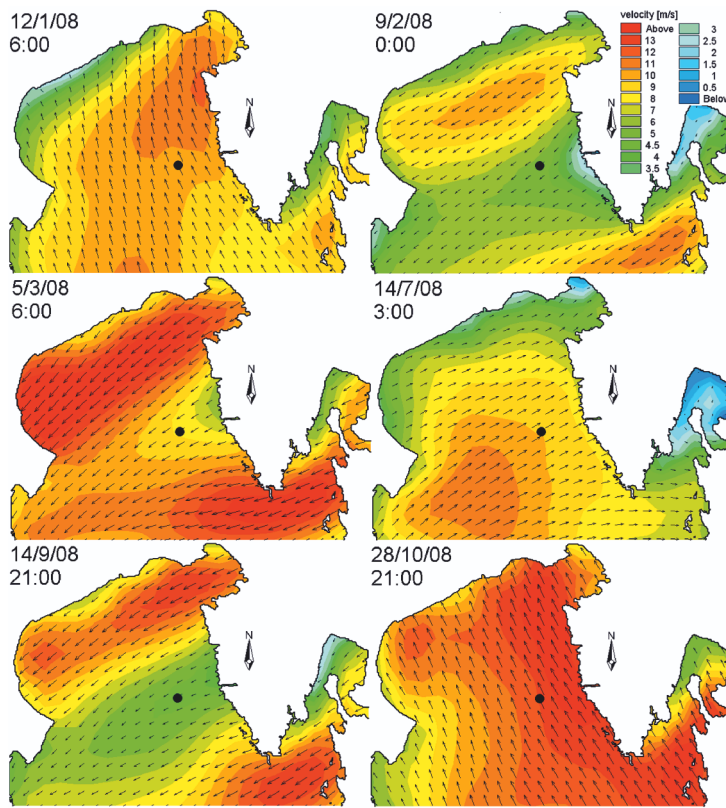


Figure 10. Model wind fields shortly after the hypothetical oil spill

The presentation of oil pollution (Figures 11–15) is given in the form of oil slick thickness [μm] and oil concentration per unit sea surface area [g m^{-2}]. The figures also give an insight into the time exposure for the first 480 hours after the onset of the spill. Time exposure should be interpreted as the time taken for a particle to be advected and dispersed from the source point to a certain location. Furthermore, the oil thickness exceeds the threshold value of 10 m throughout the simulation period of two months after the start of the oil spill, indicating the area with a longer oil retention period.

In the first situation analysed, with the oil spill starting at 18:00 hrs on 11 January 2008, the predominant circulation is under the influence of the tidal signal with the periodic exchange of NW and SE coastal circulation along the eastern coast of the area affected. The result of such a circulation is a smaller absolute shift of the oil slick and higher concentrations in the first 20 days (see Figure 11) than in the other situations addressed. An oil slick of thickness > 10 m occupies an area a little more to the north of the

spill position during 15% of the simulation period of 60 days (see Figure 11f). The oil slick reaches the coast only after 45 days, on the stretch of coastline between Rovinj and Poreč, with a maximum thickness of 5 μm .

In the first stage of the second situation analysed (the spill starts at 06:00 hrs on 6 February 2008), a NW and W circulation is predominant until the appearance of the bora (NE wind), which induces the occurrence of two eddies divided by a line along the Po-Rovinj transect. The northern eddy is characterized by a cyclonic circulation, while the southern one has an anticyclonic circulation (Supić et al. 2000, Beg Paklar et al. 2005). Thus, in the first few days, the oil slick moves westwards, after which it begins to spread intensively in the opposite E direction towards the coast of Istria, more specifically along the dividing line between the northern and southern eddies (see Figure 12e). The oil slick reaches the coast on 22 February 2008, 16 days after the oil spill. The coastal area around Rovinj is most exposed to the oil pollution, an oil slick of thickness $> 10 \mu\text{m}$ being in contact with the coastline for 3% of the total simulation period (see Figure 12f).

At the beginning of the oil spill simulation of 4 March 2008, NE and NNE winds are blowing, with a predominantly NNW circulation along the eastern coast. With such a circulation, the oil slick moves towards the north-western part of the area under investigation (see Figure 13e). The bora gains in strength until 7 March, when it reaches its maximum, again inducing the formation of two eddies. The cyclonic circulation of the northern eddy facilitates the retention of the oil slick in the central and north-western parts of the spatial domain (see Figure 13a). After the cessation of the bora, a steadier outgoing flow is established along the western coast, and consequently, removal of oil from the modelled area is intensified. The oil slick reaches the coastline 48 days after the spill (on 21 April 2008), on the stretch between Poreč and Rovinj. Retention of oil along the coastline with $> 10 \mu\text{m}$ thick layer is recorded in the following two days, that is $\approx 3\%$ of the total simulation period (see Figure 13f).

The fourth oil spill situation, of 13 July 2008, is characterized by the impact of winds from quadrants II, III and IV. A cyclonic and coastal circulation is predominant, with the pair of eddies being absent and the occurrence of the ICCC (Istrian Coastal Counter-Current). Such a circulation speeds up the removal of the oil slick from the modelled area (see Figure 14e), so that during the simulation period of 60 days no part of the coastline is exposed (see Figure 14f).

In the final oil spill situation to be analysed, dated 13 September 2008, an outgoing circulation along the western coast of Istria is predominant. The bora, blowing between 26 and 28 September 2008, does not bring about the occurrence of the cyclonic and anticyclonic pair of eddies, but

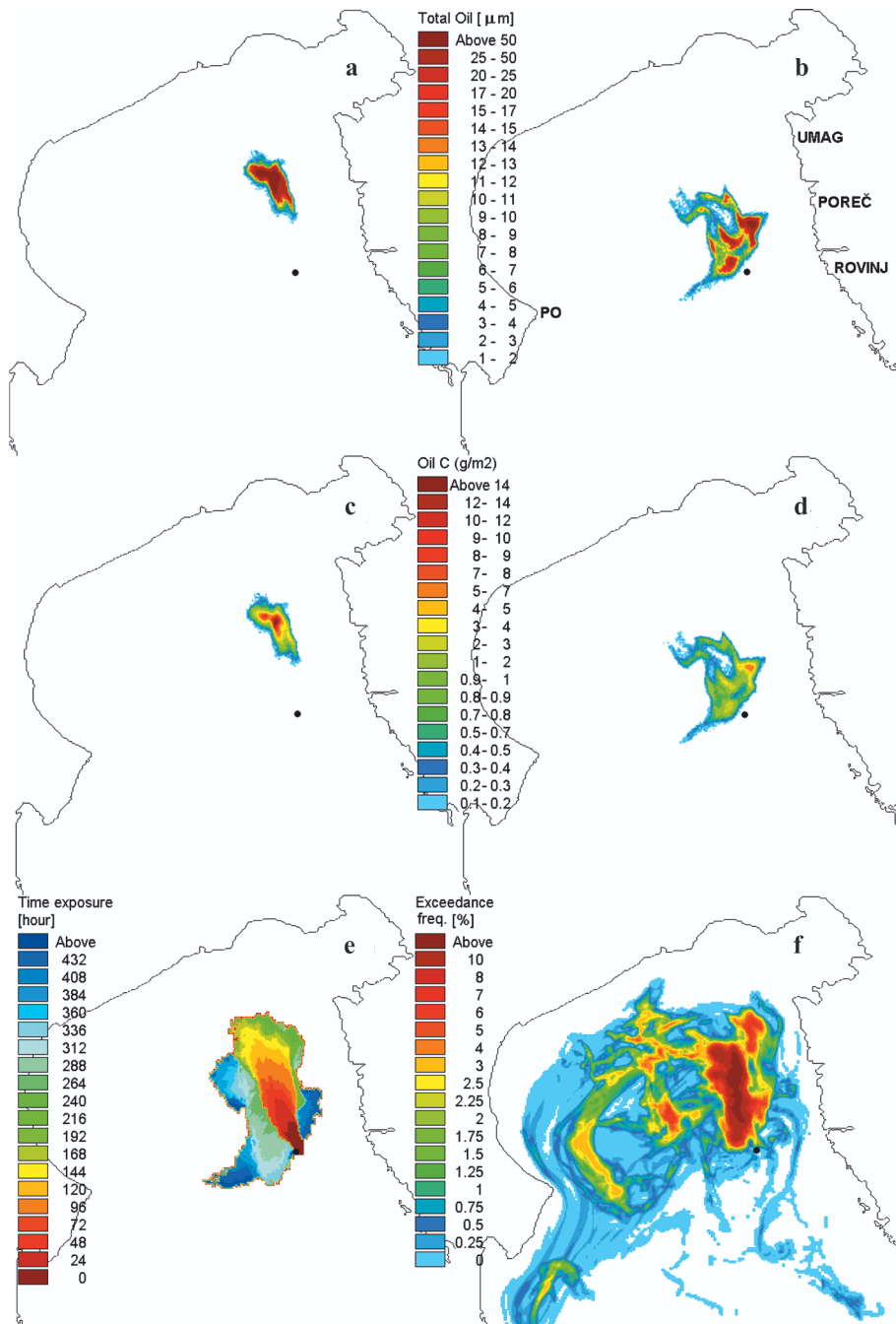


Figure 11. Oil slicks for the 240th (a, c) and 480th (b, d) hours after the onset of the spill (18:00 hrs, 11 January 2008), time exposure for the first 480 hours after the onset of the spill (e), and exceeding frequency for the threshold oil slick thickness of 10 μm for the entire simulation period of two months (f)

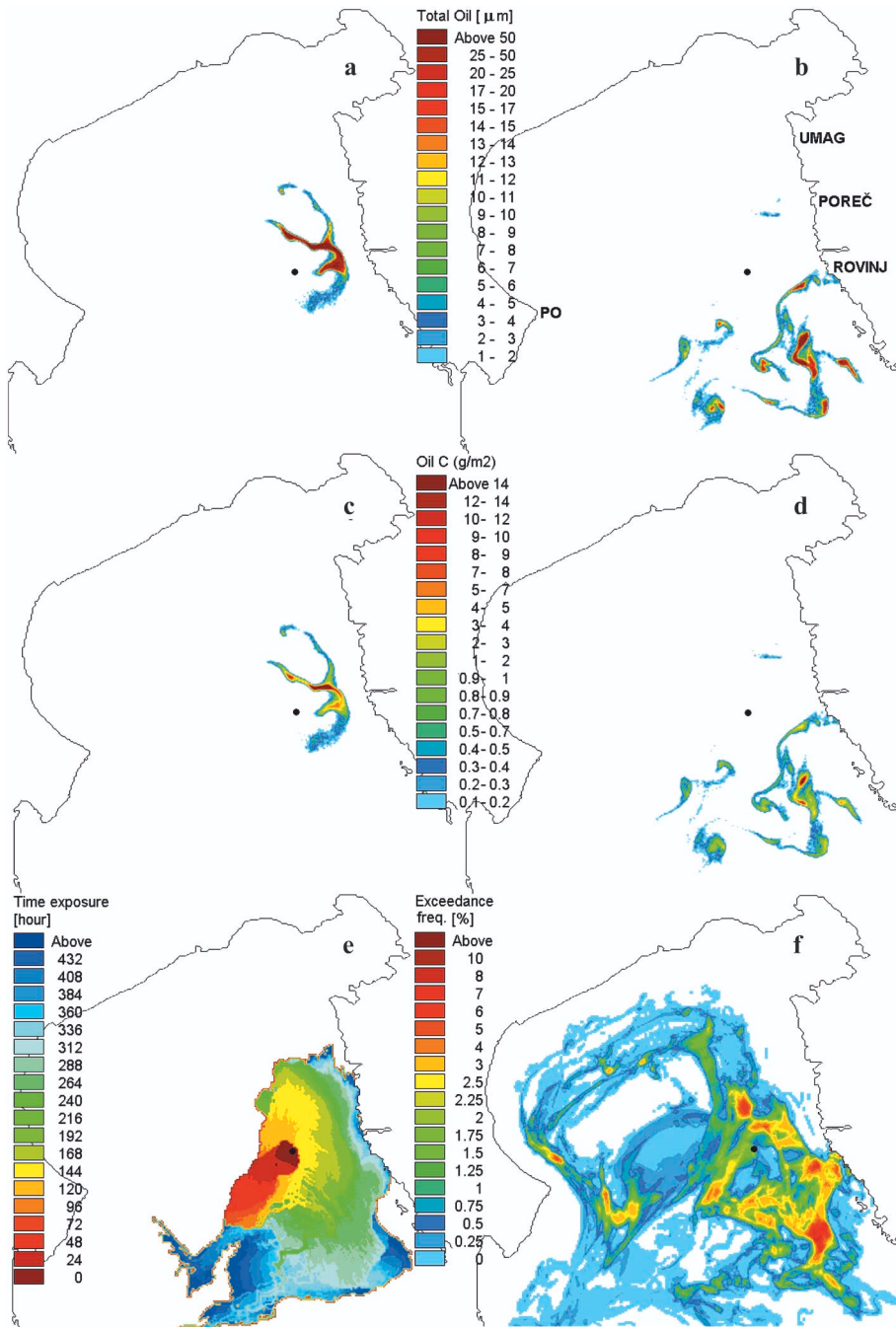


Figure 12. Oil slicks for the 240th (a, c) and 480th (b, d) hours after the onset of the spill (06:00 hrs, 6 February 2008), time exposure for the first 480 hours after the onset of the spill (e) and exceeding frequency for the threshold oil slick thickness of $10 \mu\text{m}$ for the entire simulation period of two months (f)

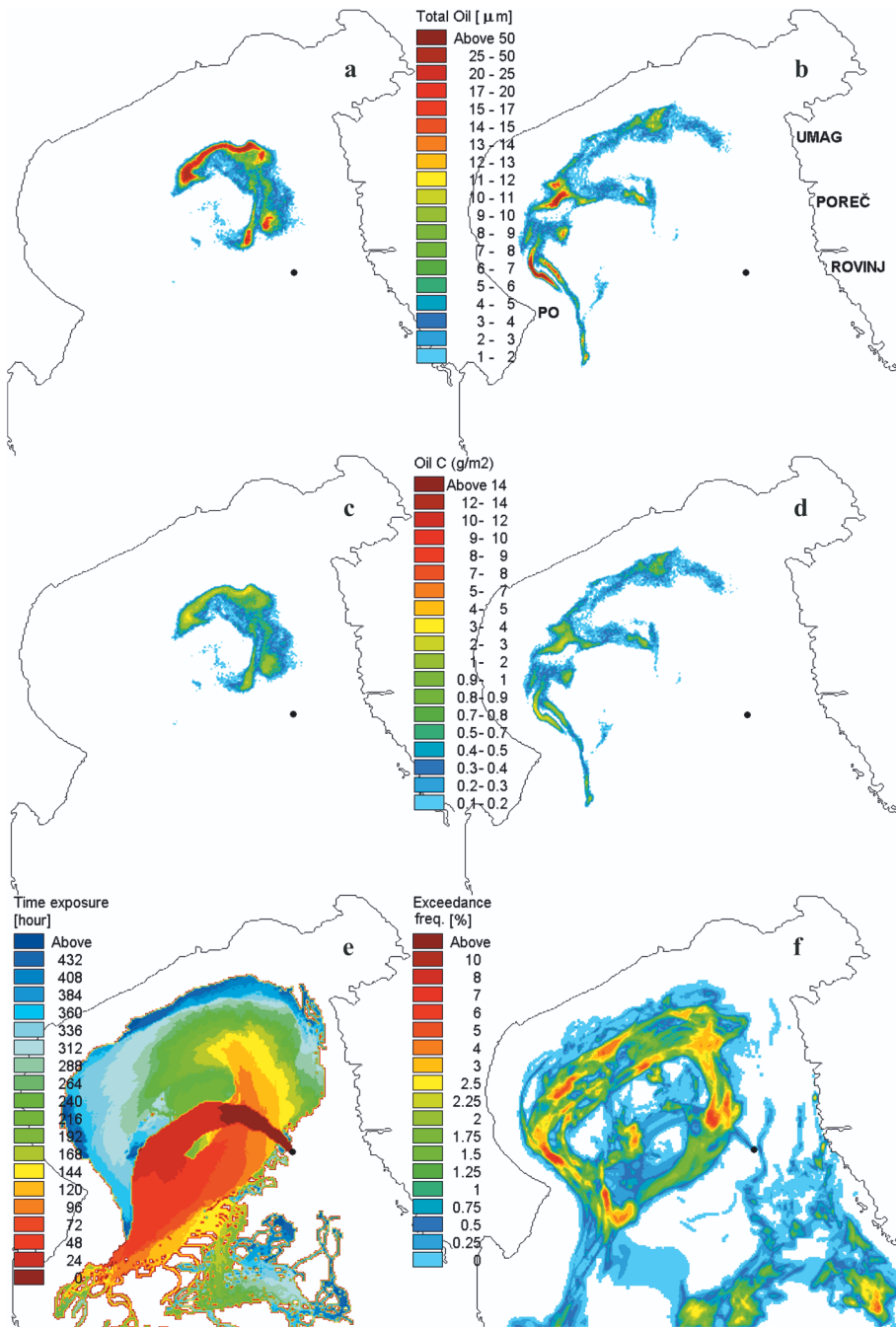


Figure 13. Oil slicks for the 240th (a, c) and 480th (b, d) hours after the onset of the spill (15:00 hrs, 4 March 2008), time exposure for the first 480 hours after the onset of the spill (e) and exceeding frequency for the threshold oil slick thickness of $10 \mu\text{m}$ for the entire simulation period of two months (f)

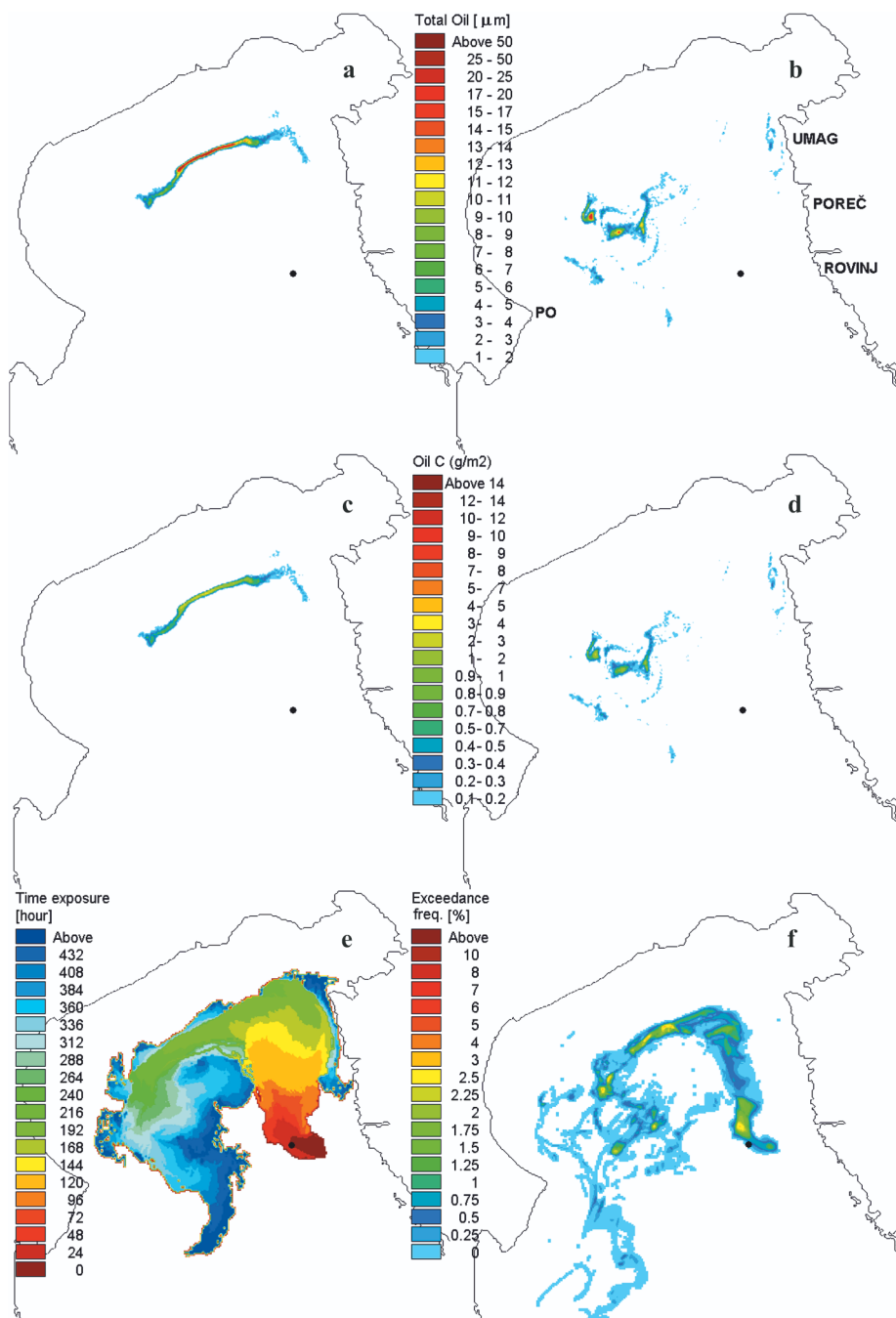


Figure 14. Oil slicks for the 240th (a, c) and 480th (b, d) hours after the onset of the spill (06:00 hrs, 13 July 2008), time exposure for the first 480 hours after the onset of the spill (e) and exceeding frequency for the threshold oil slick thickness of 10 μm for the entire simulation period of two months (f)

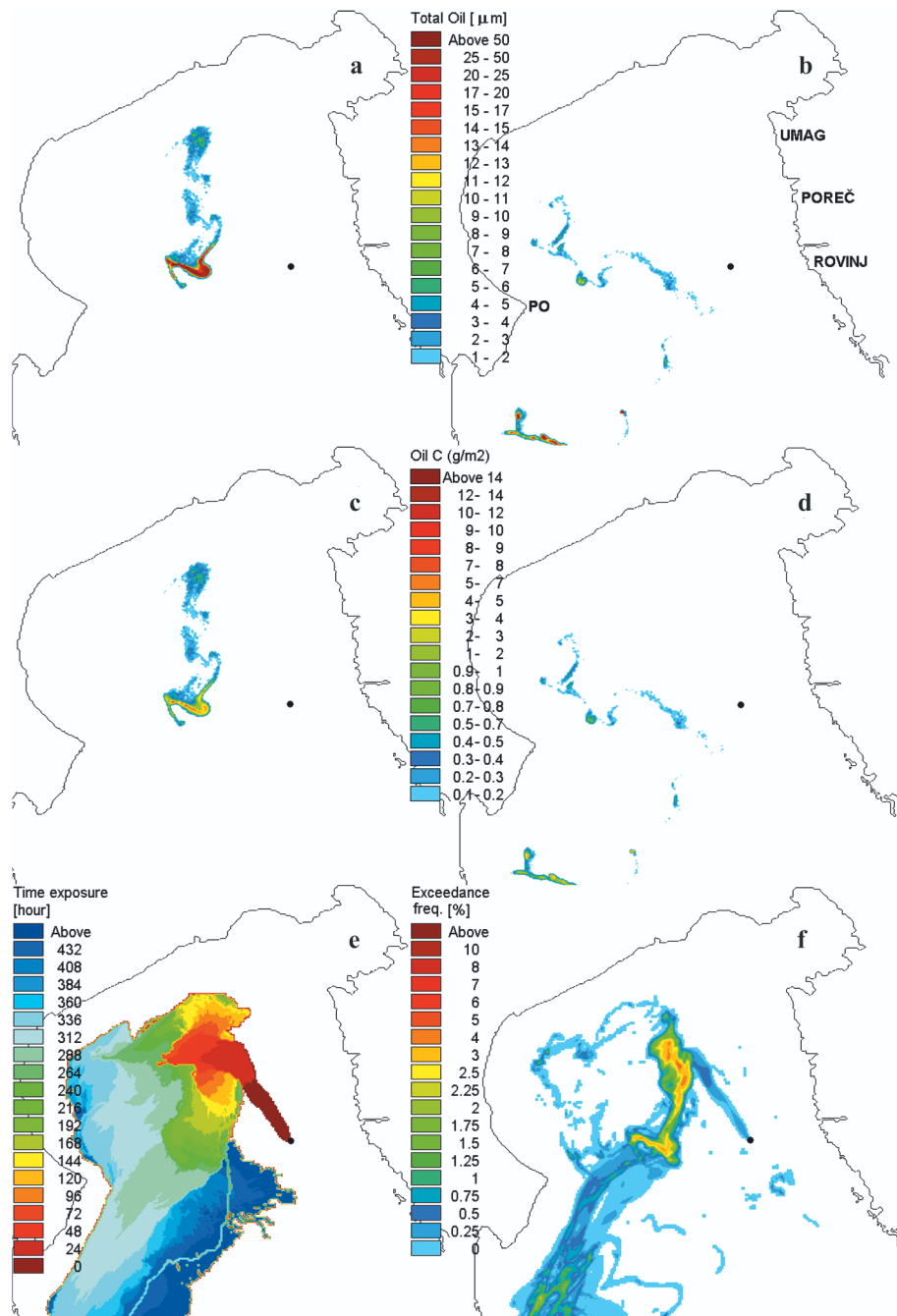


Figure 15. Oil slicks for the 240th (a, c) and 480th (b, d) hours after the onset of the spill (12:00 hrs, 13 September 2008), time exposure for the first 480 hours after the onset of the spill (e) and exceeding frequency for the threshold oil slick thickness of 10 μm for the entire simulation period of two months (f)

merely amplifies the outgoing circulation and of the removal of the oil spill along the western coast (see Figure 15e). From 2 to 4 October 2008 the impact of a libeccio (SW wind) moves the surface layer of the sea, shifting the remaining oil slick towards the central part of the model domain (see Figure 15b). After the oil has been retained in the central part of the analysed area, the oil slick spreads towards the coast, coming into contact with it on 31 October 2008. The maximum thickness of the oil slick in the area of contact with the coastline is $2 \mu\text{m}$.

The maximum length of coastline affected by oil pollution occurs in the scenario for the onset of the oil spill on 4 March 2008, followed by the scenarios on 6 February 2008 and 11 January 2008, and finally on 13 September 2008. In the case of the oil spill beginning on 13 July 2008, the shoreline is not exposed to oil pollution at all. The maximum thickness of the oil slick along the shoreline is in the same order, with values of $77 \mu\text{m}$ (scenario on 4 March), $55 \mu\text{m}$ (6 February), $33 \mu\text{m}$ (11 January) and $12 \mu\text{m}$ (13 September). The results of this simulation indicate that the stretch of coastline most endangered by a potential oil spill lies around the town of Rovinj (Figure 16). However, the western and northern parts of the Adriatic coastline (Italy) are not exposed to direct oil contamination.



Figure 16. Coastal areas that are the most exposed to oil pollution for the different times of the oil spill onset

Model results of evaporation are compared with the calculated values on the basis of empirical expressions for the following two types of crude oil: Iranian Heavy ($\text{API} = 30^\circ$) and Arabian Heavy ($\text{API} = 28^\circ$). The empirical equations $\%Ev = (2.27 + 0.045T) \ln(t)$ and $\%Ev = (2.71 + 0.045T) \ln(t)$ are used for Iranian Heavy and Arabian Heavy respectively (Fingas 2011). Parameter T is the sea temperature given in $^\circ\text{C}$, whereas t is the time elapsed since the spill, given in minutes. Figure 17 shows the time development of

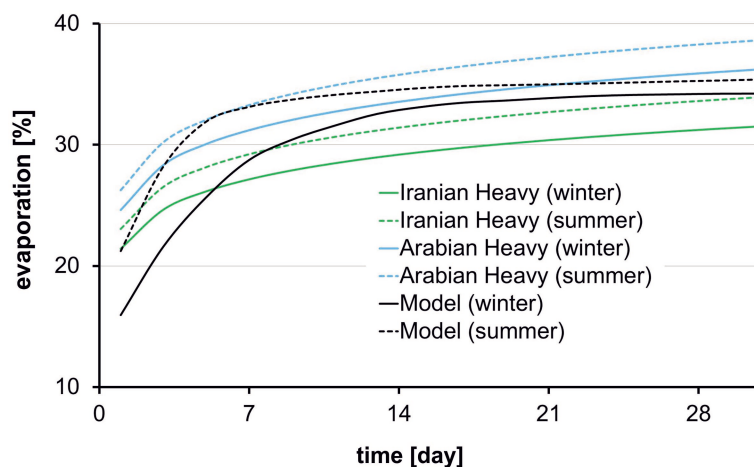


Figure 17. The time development of evaporation obtained from the model of oil spread (heavy crude oil, $\text{API} = 22.3^\circ$) and on the basis of empirical expressions (Arabian Heavy, $\text{API} = 28^\circ$; Iranian Heavy, $\text{API} = 30^\circ$). The model winter situation is based on the scenario with the oil spill occurring on 11 January 2008 and the model summer situation to the scenario with the oil spill occurring on 13 July 2008

evaporation obtained from the model of oil spread by applying the above empirical expressions.

4. Conclusions

The dynamics of physical oceanography parameters and the spread of oil in the northern Adriatic have been analysed with the aid of a numerical model. The hypothetical oil spill scenarios examined involve an oil spill due to ship failure in the position of the failure of the 'Und Adriyatik', with a continuous inflow rate of 18.5 kg^{-1} for a period of 12 hours. The oil spreading process was also analysed for the subsequent period of two months. Five hypothetical scenarios were simulated, for different times of the oil spill event. The dynamics of the parameters relating to the state of the atmosphere were adopted from the Aladin-HR prognostic atmosphere model. The model of oil spreading and the relevant reactions are based on the Lagrangian model of discrete particles with a random walk approach, using a three-dimensional current field calculated at the first step of the model's implementation. Apart from advection-dispersion, the model includes the reactive processes of emulsification, dissolution, evaporation and heat exchange between the oil, the sea and the atmosphere. The spilt oil is divided into 8 partial fractions according to its chemical structure.

This oil spill modelling shows up the great vulnerability of the Croatian coastline. In the case of an oil spill at the analysed position, the Croatian

coast is most endangered by oil pollution in the situation where the northern Adriatic double gyre current system is induced by a strong bora wind.

Modelling results indicate that the maximum concentration of oil on the coastline, presented in the form of oil-slick thickness, appears on the shoreline in the vicinity of the town of Rovinj. The maximum thickness of the oil slick on the shoreline affected by oil pollution occurs in the scenario with the oil spill onset on 4 March 2008, whereas the maximum length of coastline affected by oil pollution occurs in the scenario with the oil spill onset on 6 February 2008. On the other hand, the northern and western parts of the northern Adriatic shoreline are not exposed to oil pollution.

References

- Acta Adriatica, 2006, 47 (Suppl.), 1–266, [<http://jadran.izor.hr/acta/eng/>].
- Andročec V., Beg-Paklar G., Dadić V., Djakovac T., Grbec B., Janeković I., Krstulović N., Kupilić G., Leder N., Lončar G., Marasović I., Precali R., Šolić M., 2009, *The Adriatic Sea Monitoring Program – Final Report*, MCEPP, Zagreb, Croatia.
- Beg Paklar G., Bajić A., Dadić V., Grbec B., Orlić M., 2005, *Bora-induced currents corresponding to different synoptic conditions above the Adriatic*, Ann. Geophys., 23, 1083–1091.
- Bird R. B., Steward W. E., Lightfoot N. E., 1960, *Transport Phenomena*, Wiley and Sons, New York, 780 pp.
- Bretherton F. P., Fauday C. B., 1976, *A technique for objective analysis and design of oceanographic experiments applied to MODE-73*, Deep-Sea Res., 23, 559–582.
- Brzović N., 1999, *Factors affecting the Adriatic cyclone and associated windstorms*, Contribut. Atmos. Phys., 72, 51–65.
- Brzović N., Strelec-Mahović N., 1999, *Cyclonic activity and severe jugo in the Adriatic*, Phys. Chem. Earth Pt. B, 24, 653–657.
- CMFMWOS, 1985, *Computer model forecasting movements and weathering of oil spills – final report for the European Economic Community*, WQI & DHI.
- CONCAWE, 1983, *Characteristics of petroleum and its behaviour at sea*, Report No. 8/83, CONCAWE, Den Haag, 112 pp.
- Cordoneanu E., Geleyn J.F., 1998, *Application to local circulation above the Carpathian-Black Sea area of a NWP-type meso-scale model*, Contrib. Atmos. Phys., 71, 191–212.
- Courtier P. C., Freydier J. F., Geleyn F., Rochas M., 1991, *The ARPEGE project at METEO-FRANCE*, Proceedings from the ECMWF workshop on numerical methods in atmospheric models, 9–13 September 1991, 2, 193–231.
- Cushman-Roisin B., Gačić M., Poulain P.-M., Artegiani A., 2001, *Physical oceanography of the Adriatic Sea: past, present and future*, Kluwer Acad., Norwell, Mass, 304 pp.

- Cushman-Roisin B., Korotenko K. A., 2007, *Mesoscale-resolving simulations of summer and winter bora events in the Adriatic Sea*, J. Geophys. Res., 112 (C11), doi:10.1029/2006JC003516.
- Cushman-Roisin B., Korotenko K., Galos C., Dietrich D., 2007, *Simulation and characterization of the Adriatic Sea mesoscale variability*, J. Geophys. Res., 112 (C03S14), doi:10.1029/2006JC003515.
- Delvigne G. A. L., Sweeney C. E., 1988, *Natural dispersion of oil*, Oil Chem. Pollut., 4 (4), 281–310, doi:10.1016/S0269-8579(88)80003-0.
- DHI, 2005, *Mike 3 flow model – user guide*, DHI Water Environ. Soft., [www.dhigroup.com].
- Duffie J. A., Beckmann W. A., 2006, *Solar engineering of thermal processes*, John Wiley & Sons, New Jersey, 893 pp.
- Fay J., 1969, *The spread of oil slicks on a calm sea*, [in:] *Oil on the sea*, D. P. Hoult (ed.), Plenum Press., New York, 53–63.
- Fingas M., 2011, *Oil spill science and technology*, Elsevier-Gulf Prof. Publ., 1156 pp.
- Flores H., Andreatta A., Llona G., Saavedra I., 1998, *Measurements of oil spill spreading in the wave tank using digital image processing*, [in:] *Oil and hydrocarbon spills – modelling, analysis and control*, WIT Press, Southampton, 165–173.
- Galos C., 2000, *Seasonal circulation in the Adriatic Sea*, M.S. thesis, Dartmouth Coll., Hanover, 127 pp.,
- Gardiner C. W., 1985, *Handbook of stochastic methods: for physics, chemistry and natural science*, Springer-Verlag, Berlin, 409 pp.
- Guo W. J., Wang Y. X., 2009, *A numerical oil spill model based on a hybrid method*, Mar. Pollut. Bull., 58 (5), 726–734, doi:10.1016/j.marpolbul.2008.12.015, PMID:19157462.
- Hasselmann K., 1974, *On spectral dissipation of ocean waves due to white capping*, Bound.-Lay. Meteorol., 6 (1–2), 107–127, doi:10.1007/BF00232479.
- Hossain K., Mackay D., 1980, *Demoussifier – a new chemical for oil spill countermeasures*, Spill Technol. Newsletter, 5 (6), 154–156.
- IKU – Institut For Kontinentalsokkelundersogelser, 1984, *The experimental oil spill in Haltenbanken 1982*, IKU Publ. No. 112, Trondheim, Norway.
- IHO – International Hydrographic Organization, 1953, *Limits of oceans and seas*, Spec. Publ. No. 28, 3rd edn., IMP Monegasque, Monte Carlo, 45 pp.
- Ivatek-Šahdan S., Tudor M., 2004, *Use of high-resolution dynamical adaptation in operational suite and research impact studies*, Meteorol. Z., 13 (2), 99–08, doi:10.1127/0941-2948/2004/0013-0099.
- Janeković I., Bobanović J., Kuzmić M., 2003, *The Adriatic Sea M_2 and K_1 tides by 3D model and data assimilation*, Estuar. Coast. Shelf Sci., 57 (5–6), 873–885.
- Janeković I., Kuzmić M., 2005, *Numerical simulation of the Adriatic Sea principal tidal constituents*, Ann. Geophys., 23, 3207–3218.

- Janeković I., Sikirić-Dutour M., 2007, *Improving tidal open boundary conditions for the Adriatic Sea numerical model*, Geophys. Res. Abstr., 9, 203–217, doi:10.5194/angeo-23-3207-2005.
- Kloeden P.E., Platen E., 1999, *Numerical solution of stochastic differential equations*, Springer-Verlag, Berlin, 636 pp.
- Korotenko K., Bowman M., Dietrich D., 2010, *High-resolution numerical model for predicting the transport and dispersal of oil spilled in the Black Sea*, Terr. Atmos. Ocean. Sci., 21 (1), 123–136, doi:10.3319/TAO.2009.04.24.01(IWNOP).
- Korotenko K., Mamedov R., Kontar A., Korotenko L., 2004, *Particle tracking method in the approach for prediction of oil slick transport in the sea: modelling oil pollution resulting from river input*, J. Mar. Syst., 48 (1–4), 159–170, doi:10.1016/j.jmarsys.2003.11.023.
- Korotenko K., Mamedov R., Mooers C., 2001, *Prediction of the dispersal of oil transport in the Caspian Sea resulting from a continuous release*, Spill Sci. Technol. Bull., 6 (5–6), 323–339, doi:10.1016/S1353-2561(01)00050-0.
- Lamarre E., Melville W.K., 1991, *Air entrainment and dissipation in breaking waves*, Nature, 351, 469–472, doi:10.1038/351469a0.
- Lončar G., Ocvirk E., Androžec V., 2010, *Comparison of modelled and measured surface wind waves*, Gradevinar, 62 (3), 45–55.
- Mackay D., Bruis I., Mascarenhas R., Peterson S., 1980, *Oil spill processes and models*, Environmental protection service publication No. EE-8, Canada.
- Members of the ALADIN international team, 1997, *The ALADIN project: mesoscale modelling seen as a basic tool for weather forecasting and atmospheric research*, WMO Bull., 46, 317–324
- Morović M., Ivanov A., 2011, *Oil Spill Monitoring in the Croatian Adriatic Waters: needs and possibilities*, Acta Adriat., 52 (1), 45–56.
- Orlić M., Gačić M., La Violette P.E., 1992, *The currents and circulation of the Adriatic Sea*, Oceanol. Acta, 15, 109–124.
- Orlić M., Kuzmić M., Pasarić Z., 1994, *Response of the Adriatic Sea to the bora and sirocco forcing*, Cont. Shelf Res., 14 (1), 91–116, doi:10.1016/0278-4343(94)90007-8.
- Owens E.H., Taylor E., Humphrey B., 2008, *The persistence and character of stranded oil on coarse-sediment beaches*, Mar. Pollut. Bull., 56 (1), 14–26, doi:10.1016/j.marpolbul.2007.08.020, PMID:18001804.
- Raicich F., 1996, *On the fresh water balance of the Adriatic Sea*, J. Mar. Syst., 9 (3–4), 305–319, doi:10.1016/S0924-7963(96)00042-5.
- Rodi W., 1987, *Examples of calculation methods for flow and mixing in stratified fluids*, J. Geophys. Res., 92 (C5), 5305–5328, doi:10.1029/JC092iC05p05305.
- Science of the Total Environment, 2005, 353 (1–3), 1–380, [<http://www.journals.elsevier.com/science-of-the-total-environment/>], doi:10.1016/j.scitotenv.2005.09.007.

-
- Smagorinsky J., 1993, *Some historical remarks on the use of nonlinear viscosities*, [in:] *Large eddy simulation of complex engineering and geophysical flows*, B. Galperin & S. Orszag (eds.), Cambridge Univ. Press, 1–34.
- Supić N., Orlić M., Degobbi D., 2000, *Istrian Coastal Countercurrent and its year-to-year variability*, *Estuar. Coast. Shelf Sci.*, 51 (3), 385–397, doi:10.1006/ecss.2000.0681.
- Tkalich P., Chan E. S., 2002, *Vertical mixing of oil droplets by breaking waves*, *Mar. Pollut. Bull.*, 44 (11), 1219–1229, doi:10.1016/S0025-326X(02)00178-9.
- Wheeler R. B., 1978, *The fate of petroleum in the marine environment*, Exxon Prod. Res. Co., Houston, TX, 32 pp.
- Wu J., 1994, *The sea surface is aerodynamically rough even under light winds*, *Bound.-Lay. Meteorol.*, 69 (1–2), 149–158. doi:10.1007/BF00713300.
- Yang W. E., Wang H., 1977, *Modelling of oil evaporation in aqueous environment*, *Water Res.*, 11 (10), 879–887, doi:10.1016/0043-1354(77)90076-8.
- Zaninović K., Gajić-Čapka M., Perčec-Tadić M., 2008, *Climate atlas of Croatia 1961–1990; 1971–2000*, Meteorol. Hydrol. Service Croatia, Zagreb.
- Zore-Armanda M., Gačić M., 1987, *Effects of Bora on the circulation in the North Adriatic*, *Ann. Geophys.*, 5B, 93–102.